Non-enzymatic degradation of carbon nanotubes in the presence of bacterial enzymes

Seira Takahashi*, Fumiko Taguchi, Katsutoshi Hori*

Department of Biomolecular Engineering, Graduate School of Engineering, Nagoya University, Nagoya, Aichi 464-8603, Japan

* Corresponding authors:

takahashi.seira@b.mbox.nagoya-u.ac.jp (Seira Takahashi)

khori@chembio.nagoya-u.ac.jp (Katsutoshi Hori)

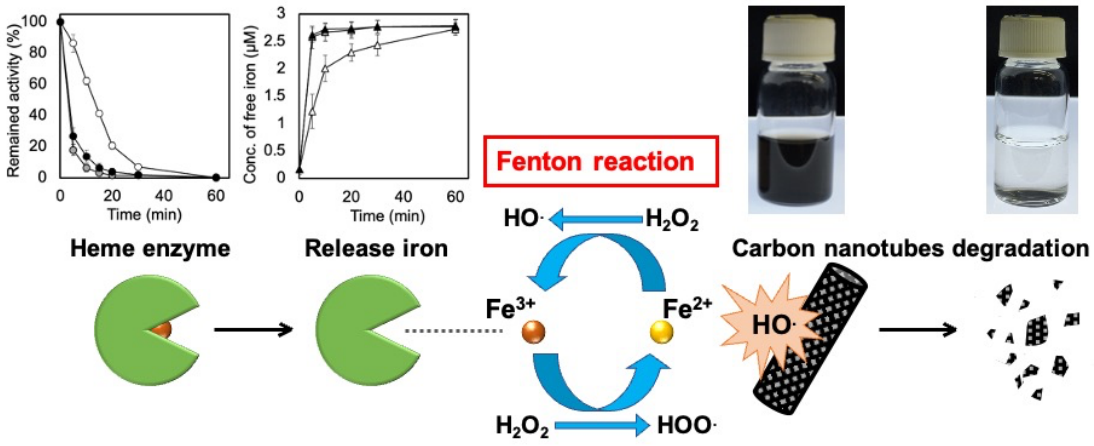

Highlights

・CNTs can be degraded in the presence of bacterial enzymes.

・Heme enzymes contribute to CNT degradation even after inactivation.

・The Fenton reaction with iron released from heme enzymes causes CNT degradation.

Abstract

The enzymatic degradation of carbon nanotubes (CNTs) by several enzymes has been reported. However, because organisms that possess these enzymes have limited habitats and distribution areas, it is unclear whether CNTs can be degraded in the general environment. The investigation of CNTs degradation by enzymes derived from bacteria, which inhabit a wide range of environments and have diverse metabolic systems, is inevitable for predicting the environmental fate of CNTs. In this study, the degradation of oxidized (carboxylated) single-walled CNTs (O-SWCNTs) by mt2DyP, a dye-decolorizing peroxidase of *Pseudomonas putida* mt-2, a common soil bacterium, was investigated. Suspensions of O-SWCNTs gradually became transparent and their optical absorbance decreased during 30 d of incubation in the presence of mt2DyP produced by a recombinant *Brevibacillus choshinensis* strain and its substrate, H_2O_2. The degradation was enhanced by higher H_2O_2 concentrations. The measurement of Raman spectra revealed the complete degradation of O-SWCNTs after 30 d of incubation with 100 mM H_2O_2. However, surprisingly, this heme enzyme was inactivated within 60 min of the incubation with O-SWCNTs, which suggested that the degradation of O-SWCNTs was not catalyzed by the enzyme. The inactivation of mt2DyP was accompanied by the release of iron, which suggested that the degradation of the O-SWCNTs was owing to the Fenton reaction caused by the iron released from mt2DyP and the supplied H_2O_2. A chelating agent, diethylenetriaminepentaacetic acid, significantly inhibited the O-SWCNTs degradation, proving the degradation by the Fenton reaction. These phenomena were also observed with another heme enzyme, Cytochrome P450. These results are important for predicting the fate of

CNTs in a wide range of environments, as heme enzymes are secreted by many bacteria in the environment. This study also shows that the effect of the Fenton reaction should be considered to validate the degradation of CNTs by heme enzymes.

Introduction

Carbon nanotubes (CNTs) have been applied in a wide range of fields such as electronics (Xiang et al., 2018), energy storage (Chen et al., 2021; Yang et al., 2019b), drug delivery (Ho et al., 2021), biosensor devices (Anzar et al., 2020; Sireesha et al., 2018; Zhao et al., 2021), and water treatment (Dong et al., 2021) owing to their excellent mechanical strength, optical properties, electrical and thermal conductivity (Dresselhaus et al., 2004). Among CNTs, single-walled CNTs (SWCNTs) have particularly excellent physical properties for application. The technology for highly efficient production of SWCNTs has been established in recent years and the problem of high production costs has been solved (Almarasy et al., 2021; Hata et al., 2004). This will lead to the expansion of the market of CNTs and the development of a wider range of applications.

With the use of CNTs becoming more widespread, the amount of CNTs released into the environment is expected to increase, either accidentally or as waste, raising concerns about their impact on human health and ecosystems. Recent studies have reported that CNTs exhibited toxicity to plants, animals, and microorganisms (Chen et al., 2018; Chen et al., 2015b; Hatami, 2017; Kumarathasan et al., 2015). However, the toxicity of CNTs depends on their length, diameter, and functionalization (Deline et al., 2020; Heller et al., 2020; Peng et al., 2020). On the other hand, the long-term safety and fate of CNTs in the environment are still poorly understood (Laux et al., 2018). CNTs may be biodegraded in the environment, and subsequent physicochemical changes can alter the original toxicity and environmental fate (Peng et al., 2020; Wang et al., 2020; Zhang et al., 2014). Therefore, it is an urgent issue to clarify the biodegradation properties of CNTs.

Since Allen et al. reported the degradation of oxidized (carboxylated) SWCNTs (O-SWCNTs),

which are functionalized SWCNTs, by horseradish peroxidase (HRP) (Allen et al., 2008; Allen et al., 2009), the biodegradation of CNTs by enzymes from several organisms, such as human myeloperoxidase (Kagan et al., 2010), human eosinophil peroxidase (Andon et al., 2013), bovine lactoperoxidase (Bhattacharya et al., 2015), fungal manganese peroxidase (Zhang et al., 2014) and lignin peroxidase (Chandrasekaran et al., 2014) has been reported. Nevertheless, the possibility of degrading CNTs by bacterial enzymes is not yet known. Bacteria have a variety of metabolic pathways, and among them there may be pathways involved in the degradation of CNTs. Bacteria can be found in any environment and there is an estimation that 1 g of soil contains 10^{10}-10^{11} bacteria (Horner-Devine et al., 2003). Therefore, it is important to investigate the degradation of CNTs by bacterial enzymes for predicting the environmental fate of CNTs.

Enzymes involved in the degradation of lignin, a huge persistent organic compound, have attracted attention for their potential to degrade other persistent organic compounds (Kadri et al., 2017; Singh et al., 2021), including CNTs (Chandrasekaran et al., 2014; Zhang et al., 2014) . Some bacteria are capable of degrading lignin as well as fungi. The dye-decolorizing peroxidases (DyPs) widely found mainly in bacteria have been studied for the ability to degrade lignin (Colpa et al., 2014; Rahmanpour and Bugg, 2015; Singh et al., 2013; Yang et al., 2018).

The purpose of this study is to clarify whether CNTs can be degraded by bacterial enzymes. We focused on enzymes from *Pseudomonas putida* mt-2, a common soil bacterium and previously reported to have a high lignin degrading ability (Bugg et al., 2011), for O-SWCNTs degradation. The findings provide essential insights for understanding the environmental fate and enzymatic degradation of CNTs.

Materials and methods

Materials

Suspensions of O-SWCNTs (Product No. ZEONANOR-SG101) was produced and provided

by Zeon Nanotechnology Co., Ltd. (Japan). 2SYN medium consisted of 2% glucose, 4% soytone, 0.5% yeast extract, 0.015% $CaCl_2 \cdot 2H_2O$, and 50 μg/mL neomycin. The pH of the 2SYN medium was adjusted at 7.2 with NaOH and H_2SO_4. Hemin chloride, 30% H_2O_2, diethylenetriaminepentaacetic acid (DTPA), 2,2'-azino-bis(3-ethylthiazoline-6-sulfonate) (ABTS), ferrozine, methanol, and acetonitrile were purchased from FUJIFILM Wako Pure Chemical Co., Ltd. (Japan).

Recombinant protein production

To produce recombinant enzymes, the *Brevibacillus* secretory expression system (TaKaRa Bio Inc., Japan) was used according to the manufacturer's instructions. Chromosomal DNA from *P. putida* mt-2 was extracted and purified using a commercial kit (Cica Geneus DNA extraction reagent, Kanto Chemical, Japan) to use for the polymerase chain reaction (PCR) as a template. The primers used in this study are listed Table 1. They consisted of a sequence (20 bases) amplifying a target gene and a 15-base 5′ overhang that was identical to the pBIC3 expression vector. The resulting PCR fragments were mixed with the plasmid vector and competent cells of *Brevibacillus choshinensis* to obtain its transformants.

Transformed cells were grown in 2SYN medium supplemented with 30 μM hemin chloride for 48 h at 30°C, and recombinant protein with an N-terminal His6-tag was extracellularly produced in the culture supernatant. After removing the cells by centrifugation, the culture supernatant was applied onto a Ni Sepharose column (Ni-Sepharose 6 Fast Flow column, GE Healthcare, Sweden), which was then washed with binding buffer (20 mM sodium phosphate, 500 mM NaCl, 20 mM imidazole, pH 7.4). The recombinant protein was eluted with elution buffer (20 mM sodium phosphate, 500 mM NaCl, 500 mM imidazole, pH 7.4). The obtained eluate was subjected to ultrafiltration using a centrifugal concentrator (Vivaspin Turbo 15, 10,000 MWCO, Sartorius, Germany) to remove imidazole and exchange buffer into ultrapure water (resistivity at 25°C, >18

MΩ·cm; TOC, <5 ppb). The recombinant protein was further purified by gel filtration using an AKTA purifier system (GE Healthcare Bio-Sciences AB, Sweden) equipped with a column (Superdex G-75, Pharmacia, Sweden), as needed. The protein sample was loaded onto the gel filtration column pre-equilibrated with 20 mM phosphate buffer (pH 7.0) and eluted with the same buffer at a flow rate of 2.0 mL/min. The fractions containing the enzyme were collected and the buffer was exchanged by ultrafiltration. All these purification steps were performed at 4°C, and the effluent from the column was monitored by absorbance at 280 nm. The protein purity was assessed by SDS-PAGE on 12.5% polyacrylamide gel. The concentration of protein was measured with a bicinchoninic acid protein assay kit (Pierce, Thermo Fisher Scientific, USA). Purified enzymes were stored at −30°C until further use.

Holoenzyme reconstitution and measurement of the enzyme activity

Holoenzymes were reconstituted by incubating purified enzyme in an aqueous solution of hemin chloride at twice the molar concentration of the enzyme for 2 h at room temperature. The excess hemin was removed by passing the mixture through a Ni Sepharose 6 Fast Flow column and imidazole in the eluate was removed in the same manner as described above. The spectral characteristics of holoenzymes were obtained using a UV-Vis spectrophotometer (Cary 60 UV-Vis, Agilent Technologies, USA). Purified and reconstituted enzymes were stored at −30°C until further use.

Enzyme activity was measured in 1 mL acetate buffer of the optimum pH for each enzyme, containing 25 μL aliquots, 0.45 mM ABTS, and 1 mM H_2O_2. The reaction was initiated by the addition of H_2O_2, and the initial rate of oxidation of ABTS at 30°C was measured at 413 nm (A_{413}). When the optimum pH of enzymes was determined, the enzyme activity for ABTS oxidation was measured in a Britton-Robinson buffer (50 mM phosphoric acid, 50 mM boric acid, and 50 mM acetic acid mixed with NaOH to the desired pH in the range 3-9) containing 0.1 μM of purified

enzyme.

Incubation O-SWCNTs with enzymes

The holoenzyme was added to the O-SWCNTs suspension diluted with ultrapure water and incubated for 24 h at 4°C in the dark, and thereafter PBS and H_2O_2 were added to initiate the reaction. The 5 mL reaction mixture contained 30 μg/mL of O-SWCNTs, 4 μM enzyme, and 1, 10, or 100 mM H_2O_2, and was incubated at 37°C in the dark for 30 d, with a daily supply of each concentration of H_2O_2 chaser. During the incubation, samples were taken periodically, an equal volume of 5% sodium dodecyl sulfate (SDS) was added for dispersion of the O-SWCNTs aggregate, sonicated for 10 min, and the absorbance at 750 nm (A_{750}) was measured to calculate the concentration of O-SWCNT from a calibration curve prepared using stocks of O-SWCNTs suspensions.

The release of free iron from holoenzymes during the incubation with O-SWCNTs was measured colorimetrically using ferrozine, following a previous method with slight modifications (Paumann-Page et al., 2013). Briefly, a 1 mL sample taken from the incubated mixture was lyophilized and resuspended in 60 μL of ultrapure water. An equal volume (60 μL) of 1.13 mM ascorbic acid solution in 0.2 M HCl was added and left for 5 min. The protein was then precipitated by adding 60 μL of 11.3% trichloroacetic acid and the samples were left on ice for 5 min followed by a short fast spin at 4 °C. To the supernatant, 72 μL of 10% ammonium acetate was added, followed by 18 μL of 6.1 mM ferrozine, and$A_{563}$was measured after 5 min (ε = 28,000 $M^{-1}cm^{-1}$).

Instrumental analyses

For Raman spectroscopy, samples were subjected to ultracentrifugation at 28000 rpm for 30 min, the supernatant was discarded by decantation, and the pellet was resuspended in methanol through sonication. Specimens were prepared by drop-casting approximately 50 μL of the samples

on a quartz microscope slide and drying. All spectra were collected on a micro-Raman spectrometer (NRS-1000, JASCO, Japan) using an excitation wavelength of 532 nm. The samples were scanned from 1000-1900 cm^{-1} to visualize the D and G bands of O-SWCNTs. Spectra were collected with a 10 s exposure time and averaged across 5 scans per sample.

To analyze the degradation products of O-SWCNTs using high-performance liquid chromatography (HPLC), 3 mL samples taken from the incubated O-SWCNTs suspension were lyophilized, resuspended in 200 μL methanol by vortexing for 1 min, and centrifuged again at 10000 rpm for 1 min. The supernatant was filtrated through a 0.22 μm membrane filter (Millex-GV, Millipore, Ireland), and 20 μL of the filtrate was injected into a HPLC system (LC-20AT, Shimadzu, Japan) equipped with a reverse-phase C18 column (InertSustain C18, 4.6 × 150 mm, 5 μm, GL sciences, Japan) and a UV detector (SPD-10A VP, Shimadzu, Japan). The mobile phase, acetonitrile solution with a linear gradient from 0% to 70% for the initial 5 min followed by 70% isocratic elution, was flowed at 1 mL/min. The detection wavelength was set to 254 nm based on the compounds identified as O-SWCNTs degradation products in a previous study (Allen et al., 2009). In liquid chromatography-mass spectrometry (LC-MS), the column and separation conditions followed HPLC analysis. Approximately 10 μL of the sample was injected into the HPLC (1200 Series, Agilent, USA) tandem mass spectrometer (Compact, Bruker Daltonics, USA) and analyzed for positive ions using electrospray mass spectrometry.

Results and discussion

O-SWCNTs degradation during incubation in the presence of DyP from *Pseudomonas putida* mt-2

First, we attempted to clone the gene encoding DyP of *P. putida* mt-2. Although the whole genome of this strain was not revealed, we found a gene homologous to E-type DyPs (PP_3248 gene; accession number, NC_002947.4) on the genome of *P. putida* KT2440, the strain that lost the

plasmid from the strain mt-2 (Regenhardt et al., 2002; Singh and Eltis, 2015). We designed PCR primers on the basis of the DNA sequence of this gene of KT2440 for the cloning of a DyP homologue from the strain mt-2, mt2DyP, and successfully obtained the amplicon by PCR using chromosomal DNA of mt-2 as a template. The DNA sequence of this amplicon was completely identical to that of the DyP gene of the strain KT2440. The cloned DNA was used for the production of the recombinant protein by *B. choshinensis.* The secreted enzyme was purified from the culture supernatant and subjected to SDS-PAGE to confirm its isolation and purity in the sample. As a result, a band was detected on the gel at ~32 kDa, corresponding to the molecular mass of mt2DyP with a 6×His tag (Fig. 1A). The reconstituted mt2DyP exhibited an absorbance maximum at 410 nm, Soret band derived from heme, with an RZ value (A_{410}/A_{280} ratio), an indicator for heme insertion, of 1.5 (Fig. 1B), which was comparable to those of DyP from other bacteria (Chen et al., 2015a; Habib et al., 2019; Rahmanpour et al., 2016). The oxidation activity of mt2DyP for ABTS, a standard substrate of peroxidase, was examined at various pH. This revealed that the enzyme activity was the highest at pH 4 (Fig. 1C), which was similar to the optimum pH values of DyPs previously reported (Chen et al., 2015a; Li et al., 2012; Roberts et al., 2011; Santos et al., 2014). Then, CNTs were incubated in the presence of mt2DyP at pH 7, which is close to the normal environment conditions to obtain useful information for predicting the environmental fate of CNTs, even though different from the optimum conditions.

A photograph of the appearance of the O-SWCNTs suspensions during incubation in the presence of mt2DyP under different H_2O_2 concentrations (1, 10, 100 mM) is shown in Fig. 2A. The black color of the O-SWCNTs decreased with the passage of time in the suspensions with 10 and 100 mM H_2O_2. Because biologically derived materials have no absorbance near 750 nm, the concentration of O-SWCNTs can be obtained by measuring A_{750} (Yang et al., 2019a), after adding SDS for removing proteins adsorbed on O-SWCNTs and dispersing the CNT aggregate. The O-SWCNTs concentrations calculated from the A_{750} values of these samples are shown in Fig. 2B. The

degradation of O-SWCNTs was more pronounced at higher H_2O_2 concentrations. The measurement of A_{750} also revealed that the O-SWCNTs degraded at 1 mM H_2O_2, although there was little change in appearance observed over time. At each H_2O_2 concentration, the control sample without mt2DyP showed a much smaller decrease in O-SWCNTs concentration than that in the presence of mt2DyP, suggesting that O-SWCNTs were slightly degraded, which may be due to trace amounts of residual iron used as a catalyst for O-SWCNTs synthesis (Hata et al., 2004). Although intrinsic catalytic iron did not contribute to the degradation of O-SWCNTs in the previous study (Allen et al., 2008), it may have contributed to the degradation in the current study owing to the high H_2O_2 concentration used in this experiment.

The degradation of O-SWCNTs was also confirmed by Raman spectroscopy. After the incubation of O-SWCNTs for 30 days in the presence of mt2DyP at a H_2O_2 concentration of 100 mM, both the G-band (graphite) peak at 1591 cm^{-1} and D-band (disordered) peak at ~1350 cm^{-1} that were present in the Raman spectra of pristine O-SWCNTs disappeared, indicating complete degradation of O-SWCNTs. (Fig. 2C).

Subsequently, the degradation products of O-SWCNTs that were produced by incubation with mt2DyP were analyzed by HPLC. After 7 days of incubation, a peak unobserved at the beginning of incubation appeared at a retention time of 3.3 min, which was expected to be the peak of an O-SWCNTs degradation product (Fig. 3A and B). To identify this degradation product, the samples were subjected to LC-MS. A mass to charge (m/z) value of 132.1 was observed only in the sample after incubation with mt2DyP (Figs. 3C and D), which corresponds to cinnamaldehyde, one of the previously reported degradation products of O-SWCNTs and pristine SWCNTs by HRP or Fenton reaction (Allen et al., 2009).

Degradation mechanism of O-SWCNTs by incubation in the presence of mt2DyP

To determine whether the enzyme really remained active during the degradation of the CNTs

for as long as a month, the enzymatic activity to oxidize ABTS of mt2DyP during incubation with O-SWCNTs was measured over time. Surprisingly, at every H_2O_2 concentration, mt2DyP was inactivated within 1 h after the start of the incubation (Fig. 4A). This implies that the degradation of O-SWCNTs was not caused by the enzymatic activity of mt2DyP.

Heme enzymes are known to be inactivated by heme degradation by H_2O_2, releasing free iron (Nagababu and Rifkind, 2004; Valderrama et al., 2002; Villegas et al., 2000). We supposed that the degradation of O-SWCNTs may have been caused by the Fenton reaction induced by iron released by the inactivation of mt2DyP. In fact, measurement of the concentration of free iron in the samples revealed its increase during incubation along with the inactivation of mt2DyP (Fig. 4B). To confirm that the degradation of O-SWCNTs was owing to Fenton reaction, incubation with mt2DyP was performed in the presence of DTPA, a chelating agent. The percentage of O-SWCNTs remaining after 30 d of the incubation in the presence or absence of DTPA as well as that of control sample without the enzyme is shown in Fig. 5. The degradation of O-SWCNTs was significantly inhibited by the addition of DTPA, which proved our hypothesis that O-SWCNTs were degraded by the Fenton reaction caused by iron released from the mt2DyP heme. However, even in the presence of DTPA, O-SWCNTs were more degraded in the sample incubated with the enzyme than in the control sample without the enzymes nor DTPA. This may be caused by a small amount of unchelated iron. Furthermore, in the control sample, O-SWCNTs was slightly degraded, which might be owing to the action of the added H_2O_2 and a trace amount of iron contaminated in water because the degraded amount increased with the H_2O_2 concentration. Importantly, the O-SWCNTs degradation observed in the presence of mt2DyP was attributed to the Fenton reaction but not to direct enzymatic reaction. This suggested that the same thing might occur in the presence of other heme enzymes.

Degradation of O-SWCNTs by incubation in the presence of another heme enzyme of *P. putida*

Cytochrome P450, a heme enzyme found in many organisms including bacteria, was examined as another heme enzyme for O-SWCNTs degradation. We designed PCR primers on the basis of the DNA sequence of Cytochrome P450 gene (PP_1955 gene; accession number, NC_002947.4) on the genome of *P. putida* KT2440 for the cloning of a Cytochrome P450 homologue from *P. putida* mt-2, mt2P450, and successfully obtained the amplicon by PCR using chromosomal DNA of mt-2 as a template. The DNA sequence of this amplicon was completely identical to that of the CytochromeP450 gene of strain KT2440, and this cloned DNA was used for recombinant protein production by *B. choshinensis*. On the gel of the SDS-PAGE of purified mt2P450, a band was detected at ~45 kDa corresponding to the molecular mass of mt2P450 with a 6×His tag (Fig. S1A). The reconstituted mt2P450 exhibited an absorbance maximum at 410 nm like mt2DyP, with an RZ value (A_{410}/A_{280} ratio) of 0.4 (Fig. S1B). Because there are no reports of the RZ value for CytochromeP450, it is impossible to evaluate the RZ value of mt2P450 in comparison with others. The ABTS oxidation activity of mt2P450 was highest at pH 5 (Fig. S1C). As expected, the incubation of O-SWCNTs in the presence of mt2P450 resulted in its degradation. As in the case with mt2DyP, when incubated with mt2P450 in the presence of 10 mM or 100 mM H_2O_2, the black color of the samples became distinctly transparent over time (Fig. 6A). The concentration of O-SWCNTs measured with A750 decreased with the incubation time, faster with higher H_2O_2 concentration (Fig. 6B). Raman spectroscopic analysis also showed that the G-band and D-band peaks in O-SWCNTs after 30 d of incubation with mt2P450 at H_2O_2 concentrations of 100 mM disappeared (Fig. 6C), which was similar to the incubation with mt2DyP. HPLC and LC-MS analyses of degradation products of O-SWCNTs by incubation with mt2P450 showed similar peaks to those observed in the case of incubation with mt2DyP (Fig. S2). The release of free iron accompanied by the inactivation of the mt2P450 enzymatic activity during incubation with O-SWCNTs was also observed (Figs. 6D and E). This proved that O-SWCNTs were degraded by the Fenton reaction caused by iron released from mt2P450, a heme enzyme other than mt2DyP, during

incubation in the presence of H_2O_2.

Although the degradation of CNTs in the environment depends on microbial activities, there have only been a few studies about the conversion or degradation of CNTs by microorganisms or their enzymes. None of these studies have led to a discussion of the degradation of CNTs in the general environment (Dai et al., 2006; Jhadav et al., 2009; Wang et al., 2020). In this study, it was found that CNTs are degraded by the Fenton reaction caused by iron released from bacterial heme enzymes. Because most bacteria secrete heme enzymes and produce H_2O_2, this result indicates that the degradation of CNTs may occur in a wide range of environments. However, the concentrations of enzymes and H_2O_2 secreted by the bacteria in the environment should be much lower than the experimental conditions in this study. Therefore, degradation of CNTs is estimated to take a very long time in the general environment. On the other hand, it was recently reported that the extracellular H_2O_2 concentration of bacteria increases in the presence of CNTs (Wang et al., 2020). Further investigation about the degradation rate of CNTs in the environment is required.

CNTs were first reported to be enzymatically degraded by HRP in a short period of time, ranging from a few days to several months (Allen et al., 2008). However, Flores-Cervantes et al. estimated the half-life of CNTs by HRP-induced degradation to be approximately 80 years (Flores-Cervantes et al., 2014). Therefore, the behavior of CNTs in degradation experiments using HRP has varied significantly, depending on the study (Russier et al., 2011; Zhang et al., 2013; Zhao et al., 2011). Previous studies have suggested that these differences may be owing to different properties of CNTs, such as surface functional groups or defects, but this is not clear (Flores-Cervantes et al., 2014; Zhang et al., 2013). However, the Fenton reaction may be the real cause of their degradation. Although all the enzymes that have been reported to degrade CNTs are heme enzymes, most of these studies have been conducted under conditions in which the effect of the Fenton reaction could not be prevented (Andon et al., 2013; Bhattacharya et al., 2015; Chandrasekaran et al., 2014). The degradation rate of CNTs can be significantly affected by the presence of small amounts of iron

released from the heme enzymes or contaminated in water, reagents, or apparatuses used in the experiment.

Conclusion

O-SWCNTs can be degraded by incubation in the presence of bacterial heme enzymes and H_2O_2. The degradation of O-SWCNTs was significantly inhibited in the presence of chelating agents, indicating that they were degraded by the Fenton reaction caused by iron released from heme enzymes during their inactivation. As heme enzymes are secreted by most bacteria, this fact provides important insights for predicting the environmental fate of CNTs. This study emphasizes that CNTs degradation experiment must be conducted under conditions that prevent the effects of the Fenton reaction.

Acknowledgement

We thank to Zeon Nanotechnology Co. Ltd for providing the O-SWCNTs sample. We also thank Mr. Kanie of Friendmicrobe Inc. (Japan) for the helpful discussion about this study.

Reference

Allen, B.L., Kichambare, P.D., Gou, P., Vlasova, I.I., Kapralov, A.A., Konduru, N., et al., 2008. Biodegradation of single-walled carbon nanotubes through enzymatic catalysis. Nano Lett. 8, 3899-3903.

Allen, B.L., Kotchey, G.P., Chen, Y.N., Yanamala, N.V.K., Klein-Seetharaman, J., Kagan, V.E., et al., 2009. Mechanistic investigations of horseradish peroxidase-catalyzed degradation of single-walled carbon nanotubes. J. Am. Chem. Soc. 131, 17194-17205.

Almarasy, A.A., Hayasaki, T., Abiko, Y., Kawabata, Y., Akasaka, S., Fujimori, A., 2021. Comparison of characteristics of single-walled carbon nanotubes obtained by super-growth CVD and improved-arc discharge methods pertaining to interfacial film formation and nanohybridization with polymers. Colloids Surf. A Physicochem. Eng. Asp. 615, 126221.

Andon, F.T., Kapralov, A.A., Yanamala, N., Feng, W.H., Baygan, A., Chambers, B.J., et al., 2013.

Biodegradation of single-walled carbon nanotubes by eosinophil peroxidase. Small 9, 2721-2729.

Anzar, N., Hasan, R., Tyagi, M., Yadav, N., Narang, J., 2020. Carbon nanotube - a review on synthesis, properties and plethora of applications in the field of biomedical science. Sensors Int. 1, 100003.

Bhattacharya, K., El-Sayed, R., Andon, F.T., Mukherjee, S.P., Gregory, J., Li, H., et al., 2015. Lactoperoxidase-mediated degradation of single-walled carbon nanotubes in the presence of pulmonary surfactant. Carbon 91, 506-517.

Bugg, T.D.H., Ahmad, M., Hardiman, E.M., Singh, R., 2011. The emerging role for bacteria in lignin degradation and bio-product formation. Curr. Opin. Biotech. 22, 394-400.

Chandrasekaran, G., Choi, S.K., Lee, Y.C., Kim, G.J., Shin, H.J., 2014. Oxidative biodegradation of single-walled carbon nanotubes by partially purified lignin peroxidase from *Sparassis latifolia* mushroom. J. Ind. Eng. Chem. 20, 3367-3374.

Chen, C., Shrestha, R., Jia, K., Gao, P.F., Geisbrecht, B.V., Bossmann, S.H., et al., 2015a. Characterization of dye-decolorizing peroxidase (DyP) from *Thermomonospora curvata* reveals unique catalytic properties of A-type DyPs. J. Biol. Chem. 290, 23447-23463.

Chen, D.R., Adusei, P.K., Chitranshi, M., Fang, Y.B., Johnson, K., Schulz, M., et al., 2021. Electrochemical activation to enhance the volumetric performance of carbon nanotube electrodes. Appl. Surf. Sci. 541, 148448.

Chen, M., Zhou, S., Zhu, Y., Sun, Y.Z., Zeng, G.M., Yang, C.P., et al., 2018. Toxicity of carbon nanomaterials to plants, animals and microbes: Recent progress from 2015-present. Chemosphere 206, 255-264.

Chen, Q.L., Wang, H., Yang, B.S., He, F., Han, X.M., Song, Z.H., 2015b. Responses of soil ammonia-oxidizing microorganisms to repeated exposure of single-walled and multi-walled carbon nanotubes. Sci. Total Environ. 505, 649-657.

Colpa, D.I., Fraaije, M.W., van Bloois, E., 2014. DyP-type peroxidases: a promising and versatile class of enzymes. J. Ind. Microbiol. Biotechnol. 41, 1-7.

Dai, Y.C., Wang, Z., Binder, M., Hibbett, D.S., 2006. Phylogeny and a new species of *Sparassis* (Polyporales, Basidiomycota): evidence from mitochondrial *atp6*, nuclear rDNA and *rpb2* genes. Mycologia 98, 584-592.

Deline, A.R., Frank, B.P., Smith, C.L., Sigmon, L.R., Wallace, A.N., Gallagher, M.J., et al., 2020. Influence of oxygen-containing functional groups on the environmental properties, transformations, and toxicity of carbon nanotubes. Chem. Rev. 120, 11651-11697.

Dong, Y.D., Zhang, H., Zhong, G.J., Yao, G., Lai, B., 2021. Cellulose/carbon composites and their applications in water treatment - a review. Chem. Eng. J 405, 126980.

Dresselhaus, M.S., Dresselhaus, G., Charlier, J.C., Hernandez, E., 2004. Electronic, thermal and mechanical properties of carbon nanotubes. Philos. Trans. Royal Soc. A 362, 2065-2098.

Flores-Cervantes, D.X., Maes, H.M., Schaffer, A., Hollender, J., Kohler, H.P.E., 2014. Slow biotransformation of carbon nanotubes by horseradish peroxidase. Environ. Sci. Technol. 48, 4826-4834.

Habib, M.H., Rozeboom, H.J., Fraaije, M.W., 2019. Characterization of a new DyP-peroxidase from the alkaliphilic cellulomonad, *Cellulomonas bogoriensis*. Molecules 24, 1208.

Hata, K., Futaba, D.N., Mizuno, K., Namai, T., Yumura, M., Iijima, S., 2004. Water-assisted highly efficient synthesis of impurity-free single-walled carbon nanotubes. Science 306, 1362-1364.

Hatami, M., 2017. Toxicity assessment of multi-walled carbon nanotubes on *Cucurbita pepo* L. under well-watered and water-stressed conditions. Ecotoxicol. Environ. Saf. 142, 274-283.

Heller, D.A., Jena, P.V., Pasquali, M., Kostarelos, K., Delogu, L.G., Meidl, R.E., et al., 2020. Banning carbon nanotubes would be scientifically unjustified and damaging to innovation. Nat. Nanotechnol. 15, 164-166.

Ho, N.T., Siggel, M., Camacho, K.V., Bhaskara, R.M., Hicks, J.M., Yao, Y.C., et al., 2021. Membrane fusion and drug delivery with carbon nanotube porins. Proc. Natl. Acad. Sci. U.S.A. 118, e2016974118.

Horner-Devine, M.C., Leibold, M.A., Smith, V.H., Bohannan, B.J.M., 2003. Bacterial diversity patterns along a gradient of primary productivity. Ecol. Lett. 6, 613-622.

Jhadav, A., Joshi, B., Ak, M., Gupta, M., Gupta, G., Patil, P., et al., 2009. Optimization of production and partial purification of laccase by *Phanerochaete chrysosporium* using submerged fermenation. Int. J. Microbiol. Res. 1, 9-12.

Kadri, T., Rouissi, T., Brar, S.K., Cledon, M., Sarma, S., Verma, M., 2017. Biodegradation of polycyclic aromatic hydrocarbons (PAHs) by fungal enzymes: A review. J. Environ. Sci. 51, 52-74.

Kagan, V.E., Konduru, N.V., Feng, W.H., Allen, B.L., Conroy, J., Volkov, Y., et al., 2010. Carbon nanotubes degraded by neutrophil myeloperoxidase induce less pulmonary inflammation. Nat. Nanotechnol. 5, 354-359.

Kumarathasan, P., Breznan, D., Das, D., Salam, M.A., Siddiqui, Y., MacKinnon-Roy, C., et al., 2015. Cytotoxicity of carbon nanotube variants: A comparative in vitro exposure study with A549 epithelial and J774 macrophage cells. Nanotoxicology 9, 148-161.

Laux, P., Riebeling, C., Booth, A.M., Brain, J.D., Brunner, J., Cerrillo, C., et al., 2018. Challenges in characterizing the environmental fate and effects of carbon nanotubes and inorganic nanomaterials in aquatic systems. Environ. Sci. Nano 5, 48-63.

Li, J., Liu, C., Li, B.Z., Yuan, H.L., Yang, J.S., Zheng, B.W., 2012. Identification and molecular characterization of a novel DyP-type peroxidase from *Pseudomonas aeruginosa* PKE117. Appl. Biochem. Biotech. 166, 774-785.

Nagababu, E., Rifkind, J.M., 2004. Heme degradation by reactive oxygen species. Antioxid. Redox Signal. 6, 967-978.

Paumann-Page, M., Furtmuller, P.G., Hofbauer, S., Paton, L.N., Obinger, C., Kettle, A.J., 2013. Inactivation of human myeloperoxidase by hydrogen peroxide. Arch. Biochem. Biophys. 539, 51-62.

Peng, Z., Liu, X.J., Zhang, W., Zeng, Z.T., Liu, Z.F., Zhang, C., et al., 2020. Advances in the application, toxicity and degradation of carbon nanomaterials in environment: A review. Environ. Int. 134, 105298.

Rahmanpour, R., Bugg, T.D.H., 2015. Characterisation of Dyp-type peroxidases from *Pseudomonas fluorescens* Pf-5: Oxidation of Mn(II) and polymeric lignin by Dyp1B. Arch. Biochem. Biophys. 574, 93-98.

Rahmanpour, R., Rea, D., Jamshidi, S., Fulop, V., Bugg, T.D.H., 2016. Structure of *Thermobifida fusca* DyP-type peroxidase and activity towards Kraft lignin and lignin model compounds. Arch. Biochem. Biophys. 594, 54-60.

Regenhardt, D., Heuer, H., Heim, S., Fernandez, D.U., Strompl, C., Moore, E.R.B., et al., 2002. Pedigree and taxonomic credentials of *Pseudomonas putida* strain KT2440. Environ. Microbiol. 4, 912-915.

Roberts, J.N., Singh, R., Grigg, J.C., Murphy, M.E.P., Bugg, T.D.H., Eltis, L.D., 2011. Characterization of dye-decolorizing peroxidases from *Rhodococcus jostii* RHA1. Biochemistry 50, 5108-5119.

Russier, J., Menard-Moyon, C., Venturelli, E., Gravel, E., Marcolongo, G., Meneghetti, M., et al., 2011. Oxidative biodegradation of single- and multi-walled carbon nanotubes. Nanoscale 3, 893-896.

Santos, A., Mendes, S., Brissos, V., Martins, L.O., 2014. New dye-decolorizing peroxidases from *Bacillus subtilis* and *Pseudomonas putida* MET94: towards biotechnological applications. Appl. Microbiol. Biotechnol. 98, 2053-2065.

Singh, A.K., Bilal, M., Iqbal, H.M.N., Raj, A., 2021. Lignin peroxidase in focus for catalytic

elimination of contaminants ? A critical review on recent progress and perspectives. Int. J. Biol. Macromol. 177, 58-82.

Singh, R., Eltis, L.D., 2015. The multihued palette of dye-decolorizing peroxidases. Arch. Biochem. Biophys. 574, 56-65.

Singh, R., Grigg, J.C., Qin, W., Kadla, J.F., Murphy, M.E.P., Eltis, L.D., 2013. Improved manganese-oxidizing activity of DypB, a peroxidase from a lignolytic bacterium. Acs. Chem. Biol. 8, 700-706.

Sireesha, M., Babu, V.J., Kiran, A.S.K., Ramakrishna, S., 2018. A review on carbon nanotubes in biosensor devices and their applications in medicine. Nanocomposites 4, 36-57.

Valderrama, B., Ayala, M., Vazquez-Duhalt, R., 2002. Suicide inactivation of peroxidases and the challenge of engineering more robust enzymes. Chem. Biol. 9, 555-565.

Villegas, J.A., Mauk, A.G., Vazquez-Duhalt, R., 2000. A cytochrome c variant resistant to heme degradation by hydrogen peroxide. Chem. Biol. 7, 237-244.

Wang, J.W., Ma, Q., Zhang, Z.J., Li, S.Z., Diko, C.S., Dai, C.X., et al., 2020. Bacteria mediated Fenton-like reaction drives the biotransformation of carbon nanomaterials. Sci. Total. Environ. 746, 141020.

Xiang, L., Zhang, H., Hu, Y.F., Peng, L.M., 2018. Carbon nanotube-based flexible electronics. J. Mater. Chem. C 6, 7714-7727.

Yang, C.X., Yue, F.F., Cui, Y.L., Xu, Y.M., Shan, Y.Y., Liu, B.F., et al., 2018. Biodegradation of lignin by *Pseudomonas* sp Q18 and the characterization of a novel bacterial DyP-type peroxidase. J. Ind. Microbiol. Biotechnol. 45, 913-927.

Yang, M., Zhang, M.F., Nakajima, H., Yudasaka, M., Iijima, S., Okazaki, T., 2019a. Time-dependent degradation of carbon nanotubes correlates with decreased reactive oxygen species generation in macrophages. Int. J. Nanomedicine 14, 2797-2807.

Yang, Z.F., Tian, J.R., Yin, Z.F., Cui, C.J., Qian, W.Z., Wei, F., 2019b. Carbon nanotube- and graphene-based nanomaterials and applications in high-voltage supercapacitor: A review. Carbon 141, 467-480.

Zhang, C., Chen, W., Alvarez, P.J.J., 2014. Manganese peroxidase degrades pristine but not surface-oxidized (carboxylated) single-walled carbon nanotubes. Environ. Sci. Technol. 48, 7918-7923.

Zhang, L.W., Petersen, E.J., Habteselassie, M.Y., Mao, L., Huang, Q.G., 2013. Degradation of multiwall carbon nanotubes by bacteria. Environ. Pollut. 181, 335-339.

Zhao, K., Veksha, A., Ge, L., Lisak, G., 2021. Near real-time analysis of para-cresol in wastewater

with a laccase-carbon nanotube-based biosensor. Chemosphere 269, 128699.

Zhao, Y., Allen, B.L., Star, A., 2011. Enzymatic degradation of multiwalled carbon nanotubes. J. Phys. Chem. A 115, 9536-9544.

Table 1 Primer sets for constructs.

Target genes	Primer sets
mt2DyP	Forward: 5'-GATGACGATGACAAAATGCCGTTCCAGCAAGGTCT-3'
	Reverse: 5'-CATCCTGTTAAGCTTTCAGGCCCGCAGCAAGGGGC-3'
mt2P450	Forward: 5'-GATGACGATGACAAAATGTCCGAAACCATTCGTGT-3'
	Reverse: 5'-CATCCTGTTAAGCTTACACGAATGGTTTCGGACAT-3'

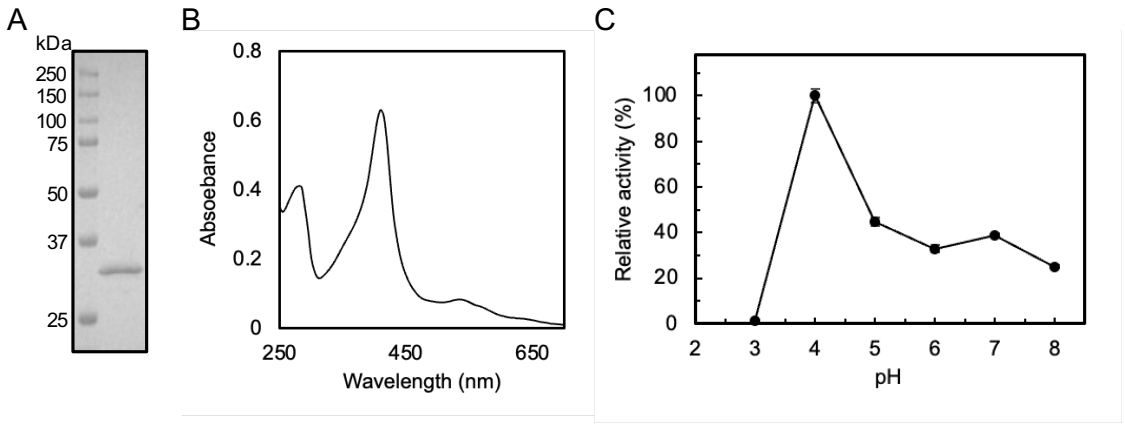

Fig. 1. SDS-PAGE (A) and UV-Vis spectrum (B) of purified mt2DyP, and the pH dependence of the enzyme activity on the ABTS substrate (C).

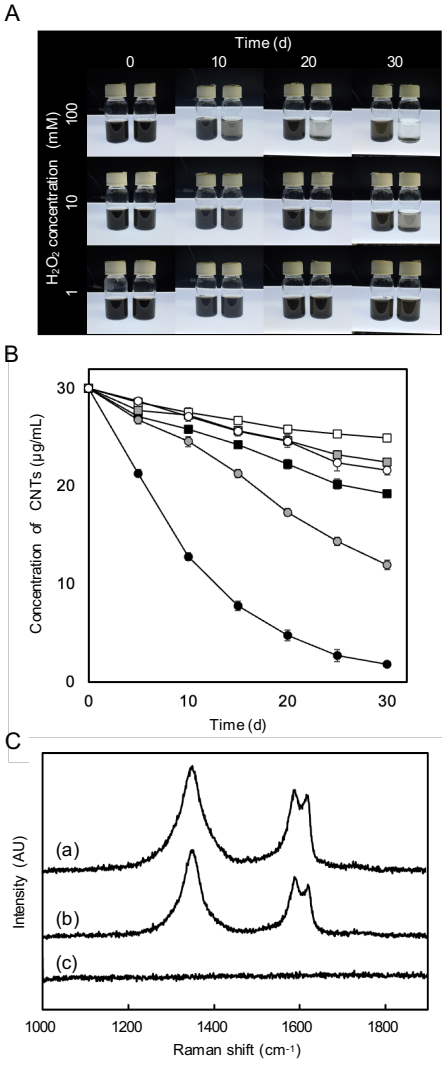

Fig. 2. Degradation of O-SWCNTs during incubation in the presence of mt2DyP under different H_2O_2 concentration conditions (1, 10, and 100 mM). (A) Photographs of the appearance of the O-SWCNTs suspensions during incubation with (right) and without (left) mt2DyP at different time points (0, 10, 20, and 30 d). (B) Time courses of CNT concentrations in its suspensions incubated with (circle) and without (square) mt2DyP. The color of the marker indicates the concentration of H_2O_2: 1 mM (white), 10 mM (gray), and 100 mM (black). (C) Raman spectra of O-SWCNTs, untreated (a) and incubated without (b) and with mt2DyP (c) at H_2O_2 concentration of 100mM for 30 d. AU, arbitrary units.

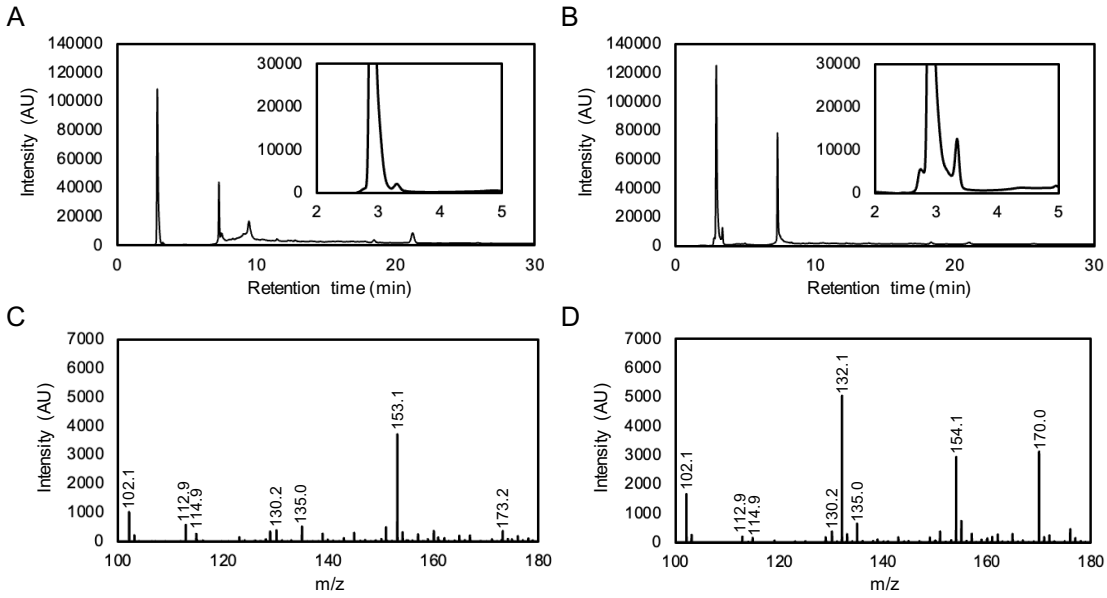

Fig. 3. Analysis of O-SWCNTs degradation products formed by incubation with mt2DyP. HPLC chromatograms of samples after 0 d (A) and 7 d (B) of incubation. LC-MS spectrum of samples after 0 d (C) and 7 d (D) of incubation. AU, arbitrary units.

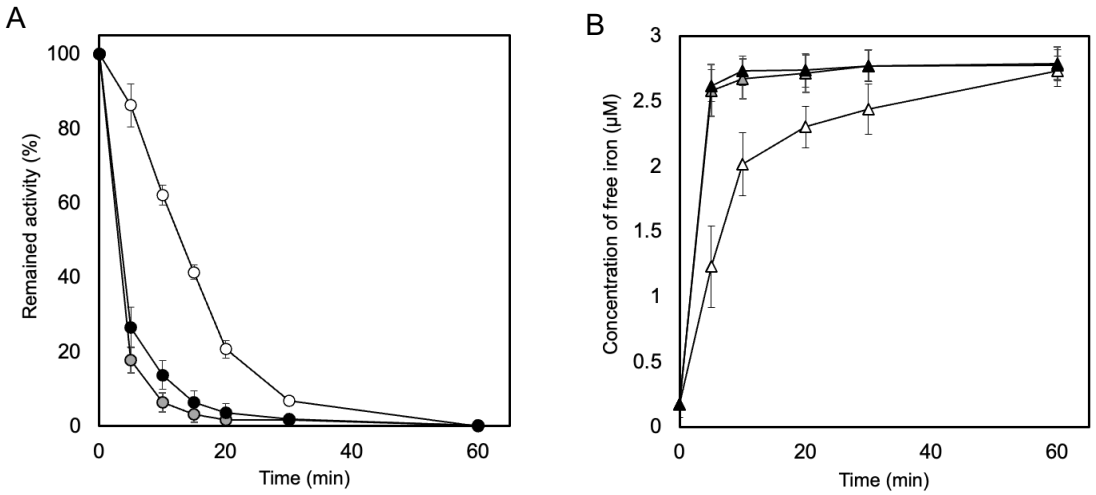

Fig. 4. (A) Time course of enzyme activity of mt2DyP during incubation with O-SWCNTs. (B) Time course of free iron concentration in samples during incubation. The color of the marker indicates the concentration of H_2O_2: 1 mM (white), 10 mM (gray), and 100 mM (black).

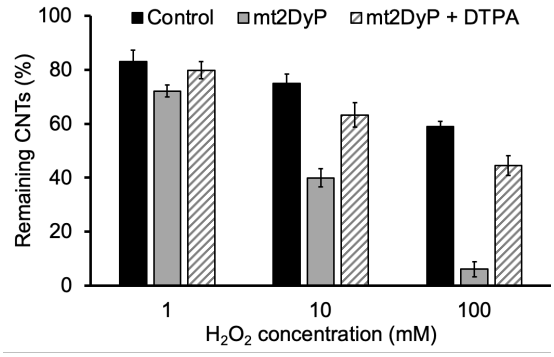

Fig. 5. Concentration of O-SWCNTs after 30 d of incubation with mt2DyP in the presence of DTPA (the initial O-SWCNTs concentration is considered to be 100%).

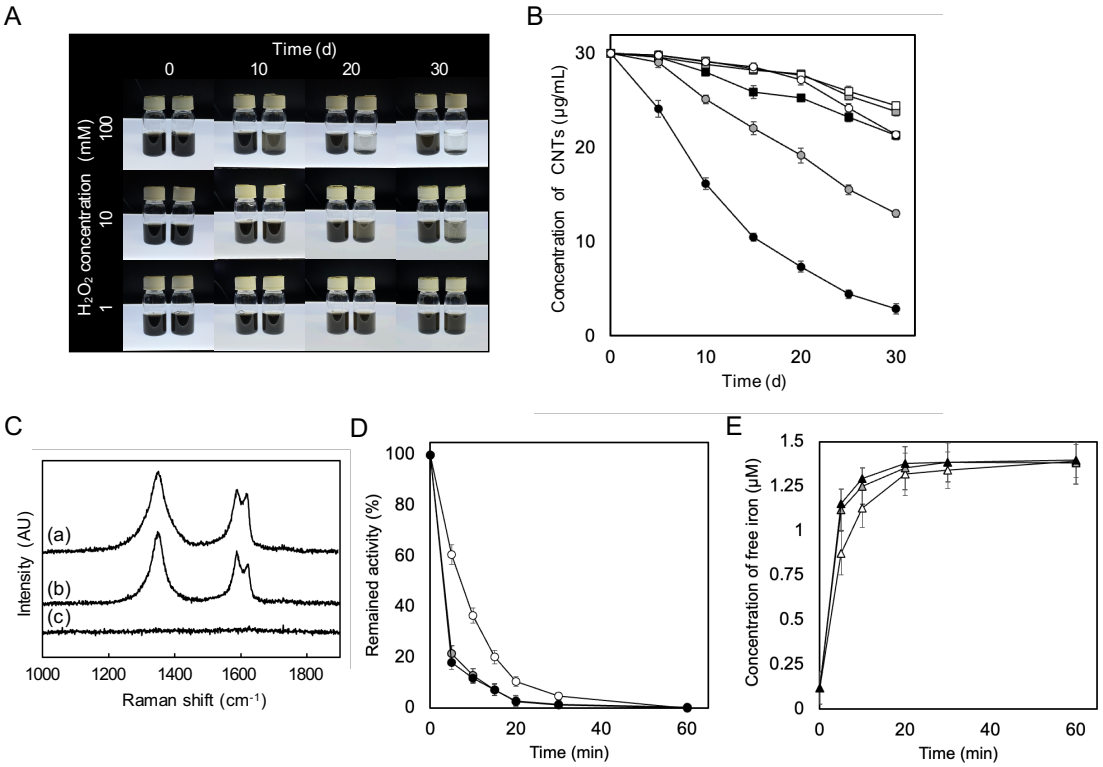

Fig. 6. Degradation of O-SWCNTs during incubation in the presence of mt2P450 under different H_2O_2 concentration conditions (1, 10, and 100 mM). (A) Photographs of the degradation of O-SWCNTs by incubation with mt2P450 (right) and without mt2P450 (left) at different time points (0, 10, 20, and 30 d). (B) Time course of the O-SWCNT concentrations in samples incubated with (circle) and without (square) mt2P450. The color of the marker indicates H_2O_2 concentration: 1 mM (white), 10 mM (gray), and 100 mM (black). (C) Raman spectra of O-SWCNTs, untreated (a) and incubated without (b) and with mt2P450 (c) at a H_2O_2 concentration of 100mM for 30 d. AU, arbitrary units. (D) Time course of enzyme activity of mt2P450 during incubation with O-SWCNTs. (E) Time course of free iron concentration in samples during incubation. The color of the marker indicates the concentration of H_2O_2: 1 mM (white), 10 mM (gray), and 100 mM (black).

Supplementary figures

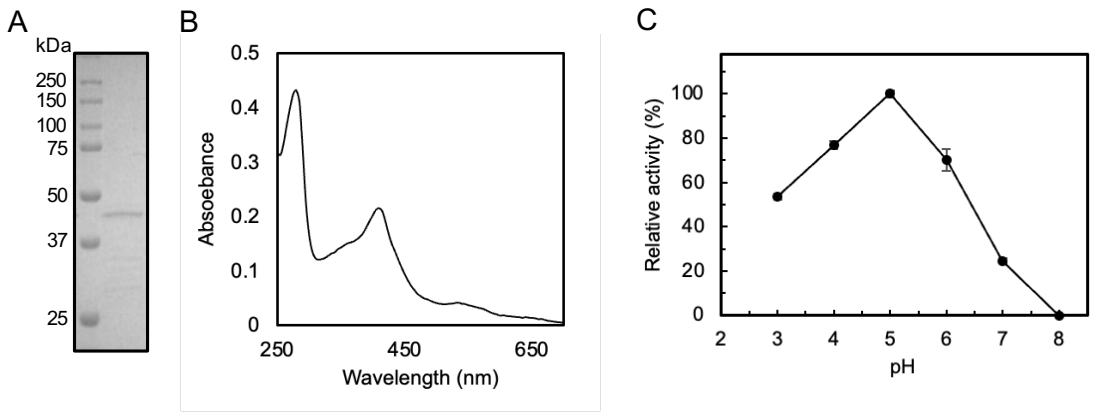

Fig. S1. SDS-PAGE (A) and UV-Vis spectrum (B) of purified mt2P450, and the pH dependence of the enzyme activity in the ABTS substrate (C).

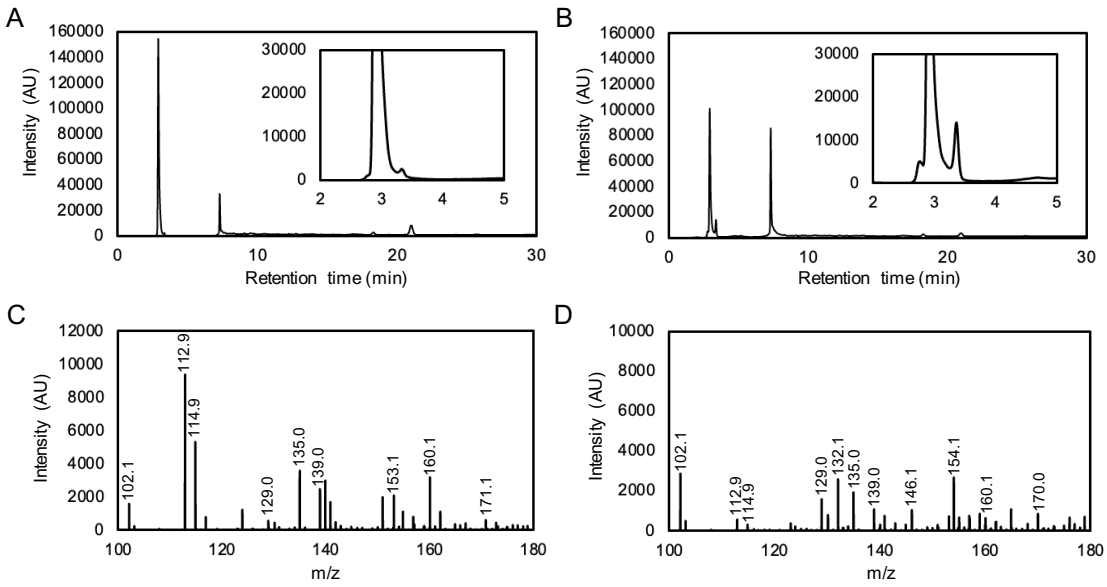

Fig. S2. Analysis of O-SWCNTs degradation products formed by incubation with mt2P450. HPLC chromatograms of samples after 0 d (A) and 7 d (B) of incubation. LC-MS spectrum of samples after 0 d (C) and 7 d (D) of incubation. AU, arbitrary units.